Supercurrent transport in $YBa_2Cu_3O_{7-\delta}$ epitaxial thin films in a dc magnetic field

Vladimir Pan,* Yuriy Cherpak, Valentin Komashko, Sergey Pozigun, and Constantin Tretiatchenko
Institute for Metal Physics, National Academy of Sciences of Ukraine, 36 Vernadsky Street, Kiev, 03142, Ukraine

Alexey Semenov and Ernst Pashitskii
Institute of Physics, National Academy of Sciences of Ukraine, 46 Nauki Avenue, Kiev 03028, Ukraine

Alexey V. Pan
ISEM, University of Wollongong, Northfield Avenue, Wollongong, NSW 2522, Australia
(Received 4 September 2005; revised manuscript received 21 December 2005; published 16 February 2006)

Magnetic field and angle dependences of the critical current density $J_c(H,\theta)$ in epitaxial *c*-oriented $YBa_2Cu_3O_{7-\delta}$ thin films are measured by the four-probe transport current technique, low-frequency ac magnetic susceptibility, and superconducting quantum interference device magnetometry. The films under study are deposited by off-axis dc magnetron sputtering onto *r*-cut sapphire substrates buffered with a CeO_2 layer. A consistent model of vortex pining and supercurrent limitation is developed and discussed. Rows of growth-induced out-of-plane edge dislocations forming low-angle boundaries (LAB's) are shown to play a key role in achievement of the highest critical current density $J_c \geqslant 2\times10^6$ A/cm^2 at 77 K. The model takes into account the transparency of LAB's for supercurrent as well as the pinning of vortex lattice on a network of LAB's. Principal statistical parameters of the film defect structure, such as the domain size distribution and mean misorientation angle, are extracted from $J_c(H)$ curves measured in a magnetic field H applied parallel to the *c* axis and from x-ray diffraction data. An evolution of angle dependences $J_c(\theta)$ with H is shown to be consistent with the model supposing dominant pinning on edge dislocations. Strongly pinned vortices parallel to the *c* axis appear to exist in tilted low magnetic fields up to a characteristic threshold field, below which the magnetic induction within the film obeys a simple relation $B=H\cos\theta$. This feature is shown to explain the absence of the expected maximum of $J_c(\theta)$ at $H\|c$ in a low applied field. A peak of $J_c(H)$ and an angular hysteresis of $J_c(\theta)$, which have been observed in an intermediate-field range, are discussed in terms of film thickness, surface quality, and orientation of the applied field. The observed effects are found to be consistent with the developed model.

DOI: 10.1103/PhysRevB.73.054508 PACS number(s): 74.25.Sv, 74.72.Bk, 74.78.Bz

I. INTRODUCTION

The highest critical current density J_c in high-temperature superconductors (HTS's) at temperature $T=77$ K is known to be reached in quasi-single-crystal $YBa_2Cu_3O_{7-\delta}$ (YBCO) *c*-axis-oriented epitaxial thin films.[1,2] A few models were proposed in order to describe J_c behavior in YBCO films in an applied magnetic field H at different orientations. The models are distinguished by the nature of pins and by the pinning mechanisms of Abrikosov vortices. The mechanisms are responsible for particular $J_c(H,\theta)$ dependences, where θ is the angle between the applied magnetic field and the film *c* axis. The most effective pinning centers are supposed to be (i) linear, extended crystal defects—cores of edge dislocations (ED's)—i.e., nonsuperconducting threads with approximately the same cross section as the coherence length in the *ab* plane ξ_{ab} (Ref. 3); (ii) planar, two-dimensional defects—twins[4] and antiphase boundaries;[5] (iii) uncorrelated (randomly distributed) pointlike defects—oxygen vacancies and/or normal phase inclusions;[6,7] and (iv) the film surface and its irregularities.[8] The measurement of angle dependences of J_c at various fields is a sensitive tool for distinguishing different pinning mechanisms and involved pinning centers. It is well known that pinning on correlated one-dimensional[9] (linear) or two-dimensional[10] (planar) defects in bulk single-crystal superconductors results in the corresponding behavior of $J_c(H,\theta)$ dependences. If extended linear and/or planar pins are aligned, a maximum of the $J_c(H,\theta)$ dependence should emerge when the direction of the applied magnetic field coincides with the direction of the aligned defects.[9,10] Such an effect was expected to be a naturally strong evidence of dominant vortex pinning on extended out-of-plane pins in HTS epitaxial thin films. However, recently Civale *et al.* have reminded us that the primary source of the $J_c(H,\theta)$ dependence variation is the anisotropic effective mass of carriers.[11] According to the anisotropic scaling approach, if pinning is provided only by an uncorrelated disorder (e.g., by random pointlike pins), the $J_c(H,\theta)$ dependence is determined by a single parameter $H(\cos^2\theta+\varepsilon^2\sin^2\theta)^{1/2}$,[12,13] where $\varepsilon=\sqrt{m_{ab}/m_c}$ is the anisotropy parameter, $\varepsilon=1/5-1/7$ for YBCO. For the monotonic decreasing $J_c(H,\theta=0)$ dependence the scaling naturally yields the $J_c(H=\text{const},\theta)$ dependence with a minimum at $\theta=0$ and a maximum at $\theta=\pi/2$.

Moreover, a maximum of the $J_c(H,\theta)$ dependence at $H\|c$ was shown (e.g., Ref. 6) to be absent for YBCO films. Ironically, many researchers considered this observation to be strong evidence for the absence of out-of-plane linear pins or their ineffectiveness for vortex pinning in epitaxial films. In a contrast, recently Maiorov *et al.* have observed the $J_c(H,\theta)$ peak at $H\|c$.[14] The maximum does exist and tends to shift

from the position at $H \| c$ for vicinal films, depending on the relationship between the anisotropy factor and the "geometry" one. Such a relationship reflects a misalignment of vortices (i.e., induction B) with respect to the external field H: $(\theta - \theta_B) \propto (d/w - \varepsilon^2)/H$,[15] where d and w are the film thickness and width (geometry), respectively, and θ_B is the angle between the magnetic induction vector and the film c axis. Silhanek *et al.* have observed the effect of misalignment for thick YBCO films at weak and intermediate fields (up to 2.5 T).[15]

Such a controversy of observed experimental results is particularly important to be clarified for finding an optimal approach to enhance the critical current density in $R\mathrm{Ba_2Cu_3O_{7-\delta}}$ materials (R is a rare-earth element), which can be used, for example, for the development of coated conductors.[14,15]

We have analyzed numerous experimental results of our previous studies,[16–18] in which a dominant contribution of extended linear defects to vortex pinning and critical current in YBCO films had become apparent, and developed a consistent model presented in this work. The out-of-plane edge dislocations, emerging during the epitaxial growth of YBCO films and forming low-angle tilt domain boundaries (LAB's) between single-crystal domains, appear to be the most effective pins for Abrikosov vortex line lattice (VLL). We show that there is no contradiction between our model and the absence of an observed maximum at $H \| c$ of $J_c(H = \mathrm{const}, \theta)$ dependences at low applied field. Moreover, the model is actually in good agreement with this observation. The present study is aimed at clarifying completely the character and evolution of $J_c(H, \theta)$ dependences in high-quality YBCO films in a wide range of orientation angles and magnetic fields.

II. EXPERIMENT

A. Deposition of epitaxial $\mathrm{YBa_2Cu_3O_{7-\delta}}$ films

Thin quasi-single-crystal YBCO films [$d \leqslant \lambda$, where $\lambda = \lambda_{ab}(T)$ is the London penetration depth] are deposited by off-axis dc magnetron sputtering (OMS).

The OMS technique and the pulse laser deposition (PLD) are known from our previous studies[3] to allow manufacturing quasi-single-crystal epitaxial YBCO films with the crystal c axis aligned perpendicularly to the film surface. A specific nanoscale network of LAB's is being formed in the film during the deposition process. The LAB's are more or less regular rows of edge dislocations (called occasionally "subgrain boundaries" or "dislocation walls"). The typical misalignment angle ϑ between neighboring domains does not exceed 1°. The characteristic domain size is 30–300 nm depending on the substrate, buffer layer, film thickness, deposition temperature, and other conditions. The YBCO is deposited at 720–740 °C in 3:1 $\mathrm{Ar/O_2}$ mixture onto r-cut single-crystal sapphire substrates with a 25–30-nm-thick $\mathrm{CeO_2}$ buffer layer deposited by rf on-axis magnetron sputtering. The growth regime of the OMS technique is much closer to a thermodynamic equilibrium comparatively with PLD. Therefore, the film growth rate during OMS of 0.01–0.02 nm/s is lower by an order of magnitude than during PLD. The structure of OMS films is much more perfect due to the quasiequilibrium growth; that is, the density of dislocations and stacking faults is also usually lower by an order of magnitude. The average density of out-of-plane edge dislocations in 300-nm-thick OMS films is about 10^{10} $\mathrm{cm^{-2}}$.

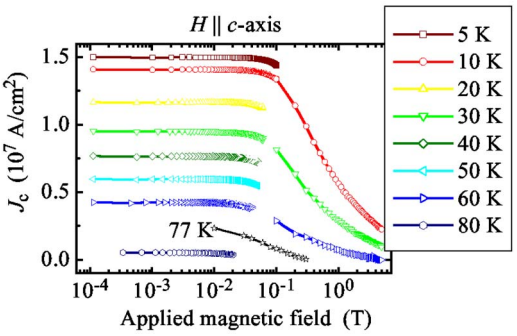

FIG. 1. (Color online) Field dependences of the critical current density for the temperature range of 5–80 K. The J_c values are extracted from the magnetization curves measured by SQUID. $J_c(H)$ measured by the four-probe transport technique at 77 K is shown for comparison.

B. Measurement techniques of the critical current density

The critical current density $J_c(T, H, \theta)$ in YBCO films is measured by three techniques: (1) superconducting quantum interference device (SQUID) magnetometry, (2) ac low-frequency magnetic susceptibility, and (3) the four-probe transport current technique.

The magnetization as a function of temperature T and applied magnetic field was measured using a Quantum Design MPMS SQUID in the field range of $|H| \leqslant 5$ T and temperature range of $5 \leqslant T \leqslant 80$ K. The critical current was calculated from the width of magnetization loops ($\Delta M = |M^+| + |M^-|$ ($|M^+|$ and $|M^-|$ are descending and ascending branches, respectively) using the critical-state model formula $J_c = 2\Delta M/\{w[1 - w/(3l)]\}$, where l is the sample length. The field dependences of the critical current measured by SQUID at different temperatures are shown in Fig. 1. It is clearly seen that the plateau regions extend to 0.02–0.10 T depending on the temperature.

The transport J_c measurements are carried out by a four-probe technique (the electric field criterion $E_c = 1$ μV/cm) using 0.25-mm-wide bridges made by conventional photolithography. The data obtained at 77 K coinciding by an order of magnitude with the SQUID measurements are shown in Fig. 1 for comparison.

The inductive contactless technique of J_c measurements is based on the recording and analysis of the imaginary part χ'' of the low-frequency magnetic susceptibility on the amplitude h_{ac} of the alternating magnetic field (937 Hz) applied perpendicularly to the film. There should be a maximum of the $\chi''(h_{ac})$ dependence at a certain $h_{ac} = h_m$.[19] The relationship between J_c and h_m for the disk samples is $J_c = 1.03 h_m/d$. This relationship is shown also to describe well

enough the results for other film geometries—for instance, a square.[20] The amplitude h_{ac} varies in the range of 0.001–5 mT. The χ'' maximum is determined using a second-order polynomial approximation of $\chi''(h_{ac})$ in the maximum vicinity. The relative error of the h_m and J_c determination does not exceed 5%.

The dc magnetic field is applied by an electromagnet with an iron yoke (0.002–1.1 T). A special sample holder with pairs of modulating and measuring coils, as well as a film sample fixed together with the coils, can rotate with respect to the applied field by 360°, preserving the film position regarding to the coil system axis. Thus, only the angle between the dc field and the film plane varies with a precision of ±0.25°. The ac magnetic field is always perpendicular to the film plane. This means that induced currents are circular and have parallel and perpendicular components with respect to the applied dc magnetic field. Therefore, such a measurement technique appears to differ from the transport measurements of $J_c(H,\theta,\varphi)$, because the angle φ between the current direction and the dc field rotation plane is indefinite. However, taking into account that $J_c(H,\theta)$ dependences for $\varphi=0$ and 90° are quite similar to each other and they may differ only a bit quantitatively,[14] the $J_c(H,\theta)$ dependences obtained by the inductive technique are expected to describe correctly the principal features of the θ dependence of J_c, in particular those connected with parallel vortice penetration into a thin film.

III. $J_c(H)$ AT TRANSVERSE AND LONGITUDINAL FIELDS

A. Transverse field

The $J_c(H\|c)$ dependences at very low fields were studied in perfect YBCO films in Refs. 16, 21, and 22. The $J_c(H\|c)$ curves—i.e., $H\perp ab$—were shown to have a plateau at $H<H_m^{\perp}$, where the critical current is approximately constant (Fig. 1). The plateau length $H_m^{\perp}$ is decreasing with increasing temperature. The following $J_c(H)$ decrease in the range $0.5<J_c(H\|c)/J_c(0)<0.9$ may be fitted well by the simple relationship

$$J_c(H\|c)/J_c(0)=\alpha\ln(H^*/H), \tag{1}$$

where α is an almost-temperature-independent parameter in the range of 0.20–0.25 for different samples.[16,17] The characteristic magnetic field $H^*=H_m^{\perp}e^{1/\alpha}$ depends linearly on the reduced temperature $\tau=1-T/T_c$. Such a character of $J_c(H\|c)$ dependences can be comprehended in a relatively simple statistical model[16,17] of VLL pinning on chains (rows) of parallel out-of-plane ED's, which form tilt LAB's between single-crystal domains randomly distributed by size.

Two competing mechanisms of the J_c limitation are considered in Refs. 16 and 17. The first one is a suppression of LAB transparency for supercurrent flow across a LAB with a relatively high misalignment angle (5°–7°). For such LAB's the superconducting "windows" separated by normal metal or dielectric dislocation cores (Fig. 2) are shrinking inversely proportional to the misalignment angle. The second one is collective depinning of the vortex lattice from a random ensemble of ED's. The critical current is determined by the mechanism providing a *lower* value at the given set of parameters. A sharp transition from the plateau to the logarithmic decrease of $J_c(H)$ observed in Refs. 16 and 17 for PLD YBCO films on (100) $LaAlO_3$ substrates is suggested to be a fingerprint of the crossover between the LAB transparency mechanism in the low field range corresponding to the J_c plateau and the collective depinning mechanism for higher magnetic fields. In a contrast, $J_c(H)$ dependences for highly perfect YBCO films, deposited by OMS onto single-crystal *r*-cut sapphire substrates buffered with a CeO_2 layer and studied in the present work, are shown to be governed by the collective depinning mechanism even at the lowest field range.

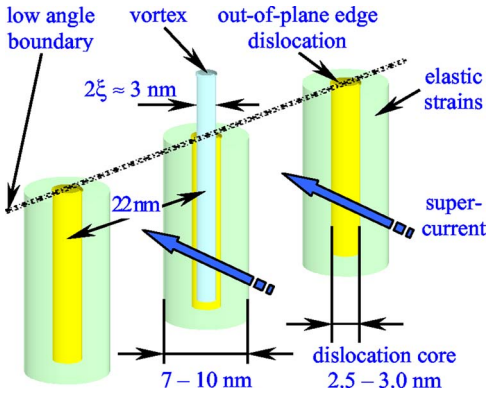

FIG. 2. (Color online) Out-of-plane edge dislocations in a low-angle (1°) domain boundary. Supercurrent is flowing across the boundary; Abrikosov vortices are pinned at dislocations.

1. Low field

A transverse magnetic field penetrates into a thin type-II superconducting film as Abrikosov vortices starting from very low fields $H>H_{c1}\sqrt{d/w}$, if there is a geometrical barrier, or $H>H_{c1}(d/w)$, if it is suppressed,[23] where H_{c1} is the first critical field for the bulk superconductor. The mean density of vortices is $n_v=H/\phi_0$—that is, the magnetic induction within the film $B\approx H$—because the film demagnetization factor is almost unity at $w\gg d$.

ED's are suggested to be the major pinning centers for Abrikosov vortices in the epitaxially grown YBCO films[16,17,24,25] and probably in some other HTS cuprates. The growth-induced ED's are perpendicular to the film plane (i.e., parallel to the crystallographic *c* axis for a *c*-axis-oriented film), threading the film throughout its whole thickness. The ED's are assumed to be the most effective vortex pins in epitaxial YBCO films since the radius of their normal core, r_0, appears to be very close to the coherence length. Moreover, the density of the "threading" ED's parallel to the vortices is proved to be extremely high and can exceed 10^{11} cm^{-2}.[25]

Estimations of the maximum pinning force[12,26] give the highest achievable value of about $f_{pin}^{max}\approx\varepsilon_0/\xi_{ab}$ for low enough temperatures, at which $r_0\approx\xi_{ab}(T)$ $(\xi_{ab}(T)=\xi_{ab}(0)\tau^{-1/2}$, $\varepsilon_0=[\phi_0/(4\pi\lambda)]^2$ is the characteristic vortex energy).

At higher temperatures, where $r_0^2 \ll \xi_{ab}^2(T)$, the energy of a vortex uniformly displaced from the center of the dislocation core by a distance u can be expressed as

$$\varepsilon_{pin}(u) \approx -\frac{\varepsilon_0}{2}\frac{r_0^2}{u^2+2\xi^2}. \quad (2)$$

Deriving by u, the force of a single vortex core pinning,

$$f_{pin}(u) = \varepsilon_0 \frac{u r_0^2}{(u^2+2\xi^2)^2}. \quad (3)$$

Thus, neglecting the proximity effect between the dislocation core and its vicinity, the maximum pinning force reached at $u=\xi\sqrt{2/3}$ is determined by the expression[26]

$$f_{pin}^{max} = \frac{9}{32}\sqrt{\frac{2}{3}}\varepsilon_0\frac{r_0^2}{\xi^3} \approx 0.23\varepsilon_0\frac{r_0^2}{\xi^3}. \quad (4)$$

At high temperatures ($T \to T_c$)—that is, at $\tau \to 0$—when $\xi_{ab}(T)$ becomes larger than the distance d between neighboring dislocations in a LAB, the pinning force is highly anisotropic with an almost free vortex sliding along the LAB's and a finite pinning force in the transverse direction. If the nanostructure of the LAB's is well ordered and has a preferential in-plane direction of the dislocation walls, an anisotropic pinning could result in the anisotropy of the critical current density. For a disordered ensemble of ED's or a random LAB network the single-vortex pinning on ED cores is supposed to determine the J_c value in accordance with the obvious relationship

$$f_{pin}^{max} = f_L = \frac{\phi_0}{c}J_c. \quad (5)$$

2. Higher fields

Let us consider now the vortex pinning mechanism at higher magnetic fields—i.e., above the low-field J_c plateau. As the applied magnetic field is increased and the distance between vortices $a=\sqrt{\phi_0/H}$ is reduced, the interaction between vortices and, therefore, the tendency to form a regular vortex lattice should be taken into account.

We suppose for simplicity that all pins (out-of-plane ED cores) are identical and their mean density n_d over the film area is much higher than the vortex density n_v. The condition $n_v \ll n_d$ is valid for an applied field of up to 2 T, provided that the average density of ED's is $n_d \approx 10^{11}$ cm^{-2}, so that the average distance between dislocations is $r_d \approx 3\times10^{-6}$ cm. However, if the out-of-plane ED's are assumed to be located primarily within LAB's separating single-crystal domains in accordance with high-resolution electron microscopy (HREM) data,[27,28] the real distance d between neighboring ED's along the LAB should be much shorter than $r_d = 1/\sqrt{n_d}$. Then, the condition $d \ll a$ should be realized in a much broader field range. For a LAB with misalignment angle $\vartheta=2°$ and $d(\vartheta) \approx 10^{-6}$ cm the condition remains valid up to 20 T.

In order to determine the critical current density in a film with a random network of LAB's, assuming that vortices and dislocations appear to be parallel to each other, the free energy loss due to the elastic distortion of VLL in the presence of linear defects has to be compared with the energy gain due to vortex pinning. Vortices should be pinned at their least possible deviations from equilibrium positions corresponding to nodes of the ideal triangular VLL. The repulsion of vortices changes essentially on the scale of λ. The vortex interaction with pinning sites is significant on the scale of ξ [Eq. (2)]. Since $\lambda/\xi=\kappa \gg 1$ ($\kappa \approx 100$ for YBCO), the interaction between dislocation cores and vortices may be approximated on a larger scale [λ and/or $a(H)$] as $\varepsilon_{pin}(u)=\varepsilon_{pin}(0)\delta(u)$ and vortices may be assumed to have two definite states: pinned with $\varepsilon_{pin}=\varepsilon_{pin}(0)$ and unpinned with $\varepsilon_{pin}=0$. In other words, the energy gain due to vortex pinning in the equilibrium state should be greater than the energy loss due to VLL strain. It is quite natural that a number of vortices remain unpinned and are in a space free of ED's—i.e., inside the single-crystal domains. The density of pinned vortices, n_p, is determined (i) by the density and spatial configuration of the pinning centers (i.e., ED cores) within a random network of LAB's, (ii) by the temperature or, more exactly, by the temperature-dependent pinning energy, and (iii) by the field-dependent VLL constant a. The ratio $n_p(H,T)/n_v(H)$—i.e., the accommodation function of distorted VLL pinned by an ensemble of ED cores—is a key characteristic of the proposed model. If there is a macroscopic current in the superconducting film, the distorted VLL is essentially rearranged. The main assumption of the model is that the accommodation function averaged over a certain macroscopic area is invariant in the presence of an applied current. Redistributed free vortices with concentration $n_v - n_p$ remain at their positions due to the electromagnetic interaction with neighboring vortices pinned by ED cores. The vortices could be rigidly pinned as a lattice if the total Lorentz force $F_L=n_v f_L=n_v\phi_0 j/c$ is compensated by the total pinning force $F_{pin}=n_p f_{pin}$, where $n_p(H,T)$ corresponds to the equilibrium without current.

Thus, the condition of collective depinning of distorted VLL from a statistical ensemble of identical pins (ED cores) determining the critical current density can be written as

$$\frac{n_p}{n_v}f_{pin}^{max} = f_L = \frac{\phi_0}{c}J_c. \quad (6)$$

The maximum pinning force is given here by Eq. (4). The ratio $n_p(H,T)/n_v(H)$ (accommodation function) is the only unknown variable for obtaining the magnetic field and temperature dependences of J_c.

The positive energy ε_d of the VLL elastic strain arising when a vortex line is displaced as a whole from its equilibrium position in VLL by a small distance δ can be described by introducing the VLL elastic shear modulus C_{66} (Ref. 12):

$$\varepsilon_d(\delta) = C_{66}(H)\delta^2, \quad C_{66} = \frac{\phi_0 H}{(8\pi\lambda)^2} = \frac{\varepsilon_0}{4a^2}. \quad (7)$$

On the other hand, the maximum absolute value of the negative potential energy for pinning on normal ED cores at the vortex displacement $u=0$ is[12,26]

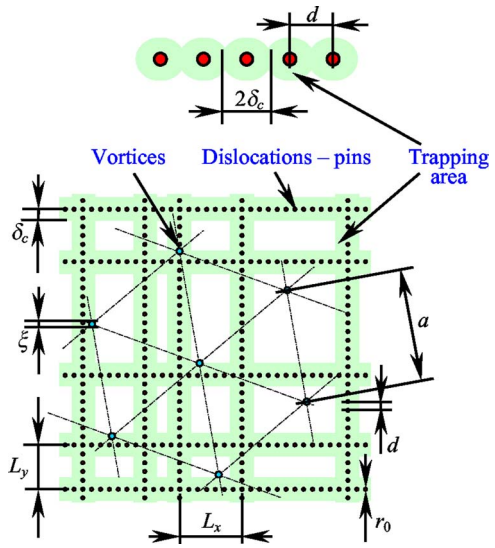

FIG. 3. (Color online) Vortex depinning model of the J_c limitation taking into account the separate action of each dislocation. Hierarchy of dimensions: $r_0 \leqslant \xi(T) < d \ll \langle L \rangle < a(H) < \lambda(T)$.

$$\varepsilon_{pin}(0) = -\frac{\varepsilon_0}{2}\ln\left(1+\frac{r_0^2}{2\xi^2}\right). \tag{8}$$

The vortex pinning is energetically beneficial if the condition $\varepsilon_v \equiv \varepsilon_d + \varepsilon_{pin} < 0$ for the vortex energy is fulfilled. Thus, the critical value of the vortex displacement δ_c, up to which the vortex remains pinned in the potential well of the ED core, is

$$\delta_c = \begin{cases} \dfrac{1}{2}a = \dfrac{1}{2}\sqrt{\dfrac{\phi_0}{H}}, & r_0 \approx 2\xi, \\ \dfrac{r_0}{\xi}\sqrt{\dfrac{\phi_0}{H}} = \sqrt{\dfrac{H_0}{H}}\tau, & r_0 < \xi. \end{cases} \tag{9}$$

If δ_c is much larger than the distance between ED's along the LAB $[d(\vartheta) \approx b/\vartheta$, where b is the Burgers vector modulus], δ_c should characterize the distance from the node of equilibrium VLL to the nearest LAB between domains. On the other hand, if the mean linear domain size $\langle L \rangle \gg d(\vartheta)$, the probability of vortex capture by one of the pinning centers should be equal to the product of probabilities of finding a VLL node inside the domain of a certain size and shape and the probability of finding it at a distance δ closer than δ_c from the domain boundary (Fig. 3).

For simplicity we suppose that all domains are random-size squares distributed by their size L as a certain statistical function $P(L)$. The normalized Γ distribution may be used:[29]

$$P(L) = \frac{\mu^\nu}{\Gamma(\nu)}L^{\nu-1}e^{-\mu L}, \tag{10}$$

where

$$\nu = (\langle L \rangle/\sigma)^2 \equiv k^2, \quad \mu = \langle L \rangle/\sigma^2 = k^2/\langle L \rangle = k/\sigma, \tag{11}$$

where σ is the dispersion of the domain size distribution function around the mean value $\langle L \rangle$. Then, the density of

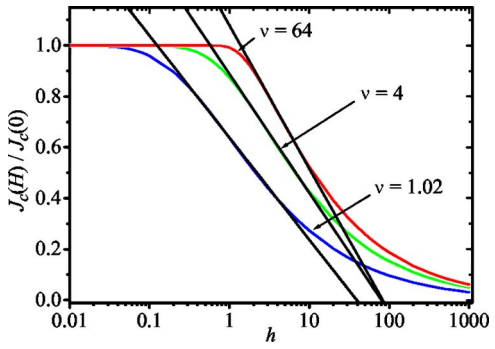

FIG. 4. (Color online) Calculated $J_c(H)/J_c(0)$ (n_p/n_v) dependences on the dimensionless parameter $h=[\nu/(2\mu\delta_c)]^2$ at different ν values. Straight lines correspond to the approximation $J_c(H\|c)/J_c(0) = \alpha \ln(H^*/H)$.

probability for a node of distorted VLL to get into a domain of linear size L is

$$W(L) = L^2 P(L). \tag{12}$$

The probability for a node to be in the δ_c-wide stripelike zone along the LAB is equal to the ratio of the stripe area to the full domain area L^2 (Fig. 3)—i.e.,

$$\tilde{P}(L,\delta_c) = \begin{cases} 1, & L \leqslant 2\delta_c, \\ 1-(L-2\delta_c)^2/L^2, & L > 2\delta_c. \end{cases} \tag{13}$$

Thus, according to Eq. (6) the critical current of VLL depinning $J_c^{depin}(H,\tau)$ normalized by the critical current of single-vortex depinning in zero field,

$$J_c^{depin}(0,\tau) = \frac{c}{\phi_0}f_{pin}^{max}, \tag{14}$$

is equal to the fraction of pinned vortices:

$$J_c^{depin}(H,\tau)/J_c^{depin}(0,\tau) = n_p(H,\tau)/n_v(H). \tag{15}$$

Taking into account Eq. (13) the following expression for the accommodation function is obtained:

$$\frac{n_p}{n_v} = \int_0^{2\delta_c} W(L)dL + \int_{2\delta_c}^{\infty} W(L)\left[1-\frac{(L-2\delta_c)^2}{L^2}\right]dL, \tag{16}$$

where $W(L)$ is determined by Eq. (12). The effect of magnetic field is involved only through the dependence $\delta_c(H) \propto 1/\sqrt{H}$. Integrating Eq. (16) for the Γ distribution,

$$\frac{n_p}{n_v} = 1 - \frac{1}{\Gamma(2+\nu)}[4\mu^2\delta_c^2\Gamma(\nu,2\mu\delta_c) - 4\mu\delta_c\Gamma(1+\nu,2\mu\delta_c) + \Gamma(2+\nu,2\mu\delta_c)], \tag{17}$$

where $\Gamma(x)$ and $\Gamma(x,\alpha)$ are complete and incomplete Euler's Γ functions.

The calculated n_p/n_v dependences on the dimensionless parameter $h=[\nu/(2\mu\delta_c)]^2$ are plotted in Fig. 4 for different ν values corresponding to different relative widths of the do-

main size distribution [Eq. (11)]. The dependences well describe the measured $J_c(H)$ for epitaxial YBCO films in a wide field range.

It is worth noting that the whole film area cannot be filled homogeneously with square domains arbitrarily distributed by size. The simplest complete filling can be achieved using rectangular domains with independent random distributions of their two dimensions L_x and L_y. The total distribution can be described by the product of $P(L_x)$ and $P(L_y)$ functions in the form of Eq. (10). In this case, the probability of vortex capture by one of the dislocation potential wells in the boundary of the $L_x \times L_y$ domain is

$$\tilde{P}(L_x, L_y, \delta_c) = \begin{cases} 1, & L_{min} \leqslant 2\delta_c, \\ 1 - \dfrac{(L_x - 2\delta_c)(L_y - 2\delta_c)}{L_x L_y}, & L_{min} > 2\delta_c, \end{cases} \tag{18}$$

where $L_{min} = \min(L_x, L_y)$. The fraction of pinned vortices is[17]

$$\frac{n_p}{n_v} = 1 - \frac{1}{\Gamma^2(\nu)}[\Gamma(\nu, 2\mu\delta_c) - 2\mu\delta_c\Gamma(\nu - 1, 2\mu\delta_c)]^2. \tag{19}$$

In spite of the essential difference between analytical expressions (17) and (19), the corresponding field dependences turn out to be very similar for the same ν value. The discrepancy of the curves at the inflection point does not exceed 5%. This means a comparatively weak effect of domain shape on the field dependence of the critical current density.

The discretion of LAB's, which consist of dislocations with normal cores separated by the distance d, should be taken into account for a good quantitative description of the experimental $J_c(H)$ curves at an applied field above 1 T.[18,22,30] This can be done by introducing a geometrical factor $f(d/(2\delta))$,

$$f(x) = \frac{1}{2}[\sqrt{1 - x^2} + \arcsin x/x], \quad \text{for } x < 1,$$

$$f(x) = \pi/(4x), \quad \text{for } x = d/(2\delta) > 1, \tag{20}$$

into the probabilities (13) and (18). In the case of rectangular domains the expression for n_p/n_v should be as follows:

$$\frac{n_p}{n_v} = 1 - \left[1 - f\left(\frac{d}{2\delta_c}\right)\right]\left[\frac{\Gamma(\nu, 2\mu\delta_c)}{\Gamma(\nu)}\right]^2 - f\left(\frac{d}{2\delta_c}\right)\left[\frac{\Gamma(\nu, 2\mu\delta_c) - 2\mu\delta_c\Gamma(\nu - 1, 2\mu\delta_c)}{\Gamma(\nu)}\right]^2. \tag{21}$$

It is easy to see that at low fields ($\delta \to \infty$) the geometrical factor [Eq. (20)] tends to unity and Eq. (21) is reduced to Eq. (19). At higher fields Eq. (21) provides an asymptotic behavior $J_c \propto H^{-1}$ consistent with the experimental data.[18,22]

The critical current normalized by the plateau value follows from the model to depend on the magnetic field and temperature only through the parameter $\delta \propto (\tau/H)^{1/2}$. This means that $J_c(H \| c, T)/J_c(0, T)$ should be invariant upon δ;

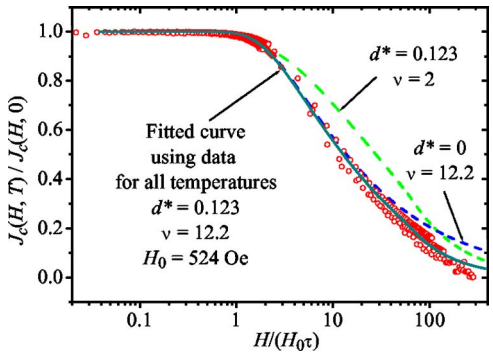

FIG. 5. (Color online) Reduced field dependences of the critical current density. The solid line is the fitted curve using data for 10, 30, and 60 K (Fig. 1). Dashed lines are calculated dependences for a wide distribution (ν=2) and for continuous boundaries (d=0). $d^* = d/\langle L \rangle$.

i.e., the plots of normalized J_c versus $H/(H_0\tau)$ for different fixed temperatures must coincide [the characteristic field H_0 is introduced for convenience from the condition $2\mu\delta \equiv \nu(2\delta/\langle L \rangle) \equiv \nu(H_0\tau/H)^{1/2}$—i.e., $H_0 = 8r_c^2\phi_0/(\xi_0^2\langle L \rangle^2)$, where r_c is the radius of nonsuperconducting dislocation core]. This is the case with good precision for the data shown in Fig. 1. The experimental data have been fitted by Eq. (21) with H_0, ν and $d/\langle L \rangle$ chosen as independent parameters (Fig. 5). A slight deflection from the universal fit for high temperatures and fields is observed. This may be caused by a flux creep,[12] since the creep rate is increasing with temperature and decreasing with critical current.

The value of $\nu \approx 12$ obtained by the fitting procedure corresponds to a rather narrow domain size distribution. The parameter $\alpha = \partial[J_c(H)/J_c(0)]/\partial \ln(H_0\tau/H)$ at the inflection point is estimated to be 0.25, which is higher than in Ref. 17, where α was in the range of 0.18–0.24. Assuming $r_c = 0.5\xi_0$, the mean domain size estimated from the fit value of H_0=524 Oe is $\langle L \rangle$=280 nm. The third fitting parameter $d \approx 35$ nm. The domain misalignment angle ϑ estimated using Frank's relationship is 0.65°.

The domain size distribution can be also derived from the Fourier coefficients of the x-ray reflection profile in an appropriate direction—that is, with a nonzero component in the *ab* plane. The original line shape is taken into account by a reference reflection (for example, from the sapphire substrate). Lattice strains can be excluded by recording two orders of the same reflection. In particular, we used (1 0 6) and (2 0 12) reflections. According to the Warren-Averbach (WA) procedure[31] the domain size distribution is proportional to the second-order derivative of the Fourier transformation of the x-ray diffraction line profile. Unfortunately, the WA procedure suffers from very high sensitivity to spurious oscillations of the transformation, which lead to doubtful oscillations of the distribution curves. Therefore, in order to compare the domain size distribution extracted from x-ray data with that obtained from the field dependence of the critical current we fitted the first derivative of the Fourier transformation to the predicted one in the assumption of a Γ distribution using a conventional simplex procedure. Taking into account the model roughness, the obtained values

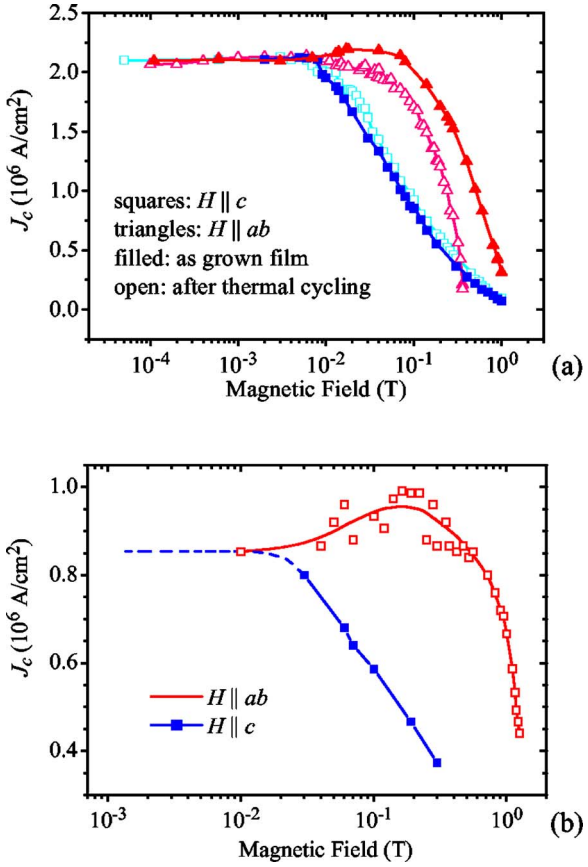

FIG. 6. (Color online) $J_c(H)$ dependences at 77 K for parallel and perpendicular applied fields for 300-nm-thick OMS YBCO films (a) K2 measured by the ac magnetic susceptibility technique and (b) K6300 measured by the four-probe technique.

$\nu \approx 8$ and $\langle L \rangle = 220$ nm are in sufficient agreement with estimations from magnetic measurements.

B. Longitudinal field

The $J_c(H \| ab)$ dependences shown in Fig. 6(a) are measured for the OMS YBCO film (K2) by the ac magnetic susceptibility technique and using a Clem-Sanchez analysis of $\chi''(h_{ac})$ data.[19] Similar results are obtained for another OMS YBCO film (K6300) by the transport four-probe technique [Fig. 6(b)].

The $J_c(H \| ab)$ dependences for parallel (longitudinal) fields also reveal a plateau at $H < H_m^{\|}$ (Fig. 6). However, the following important peculiarities should be noted.

(i) The $J_c(H \| ab)$ at the plateau appears to be *exactly* equal to $J_c(H \| c)$.

(ii) The $J_c(H \| ab)$ plateau is much longer than for $H \| c$—i.e., $H_m^{\|} > H_m^{\perp}$.

(iii) A $J_c(H \| ab)$ enhancement (peak effect) is observed for the most perfect films at 77 K just above the plateau and before the following $J_c(H)$ decrease.

(iv) The peak effect disappears and the $J_c(H \| ab)$ decreasing branch above $H_m^{\|}$ shifts towards the $J_c(H \| c)$ dependence after thermal cycling—i.e., heating up to 300 K and cooling down to 77 K.

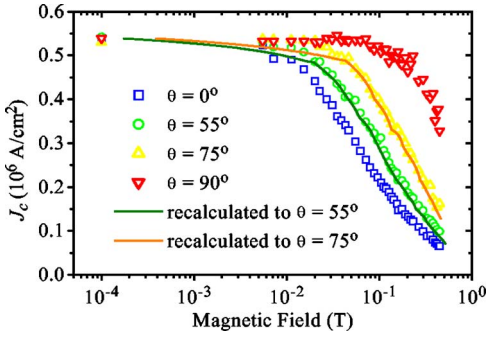

FIG. 7. (Color online) $J_c(H)$ dependences for the OMS film K34-2 (32 nm thick) for various magnetic field orientations, measured (symbols) and recalculated according to Eq. (22) (solid curves).

(v) The $J_c(H \| ab)$ decrease following the plateau is much steeper than for $H \| c$.

(vi) The steeper decrease of $J_c(H \| ab)$ results in a crossing of the $J_c(H, \theta = 0°)$ and $J_c(H, \theta = 90°)$ dependences at a certain characteristic field H_{cr}.

The curves plotted by solid symbols in Fig. 6 and both curves in Fig. 6(b) are measured for as-grown YBCO films. The critical current density for the K2 film after several thermal cycles between 300 K and 77 K is shown in Fig. 6 with open symbols. The $J_c(H \| ab)$ dependences essentially change after thermal cycling. The plateau length $H_m^{\|}$ decreases and the maximum disappears. In a contrast, the $J_c(H \| c)$ dependence remains unchanged.

The $J_c(H \| ab)$ peak effect and its disappearance after thermal cycling can be comprehended by consideration of the surface barrier (similar to the well-known Bean-Livingston barrier) preventing entry and exit of vortices parallel to the surface of superconductor. The thermal cycling is supposed to result in film surface degradation and hence in surface barrier reduction. The surface degradation affecting only a thin surface layer is unable to deteriorate substantially the transport properties of the film as a whole, but it may result in the disappearance of the J_c maximum. The influence of the film surfaces on film properties is considered in more detail in the Discussion.

C. Arbitrarily inclined field

The $J_c(H)$ dependences in an external dc field applied at an arbitrary angle θ to the c axis also reveal a J_c plateau at $H < H_m(\theta)$. This observation does not depend on the measurement technique. A few very interesting peculiarities of the $J_c(H)$ behavior should be noted. (i) The plateau length $H_m(\theta)$ may increase from $H_m^{\perp}$ to $H_m^{\|}$ with θ in accordance with the change of the perpendicular field component $H^{\perp} = H \cos \theta$. (ii) Figure 7 shows that for a wide range of angles $(0 < \theta < 60° - 70°)$ and fields $(H_m^{\perp} < H < H_m^{\|})$ the $J_c(H)$ curve should be well described by a logarithmic law similar to Eq. (1) if the applied field H is substituted by its perpendicular component $H^{\perp}$. (iii) For OMS YBCO films with a very smooth surface the $J_c(H \| ab)$ peak effect is observed in a rather wide range of angles near $\theta = 90°$ at fields higher

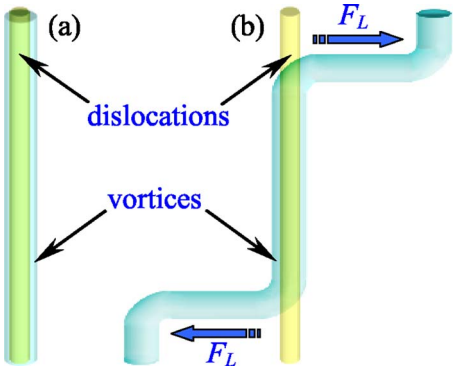

FIG. 8. (Color online) Bending of vortices partly pinned on ED cores. (a) Completely pinned vortex. (b) Vortex with depinned ends under the action of Meissner current.

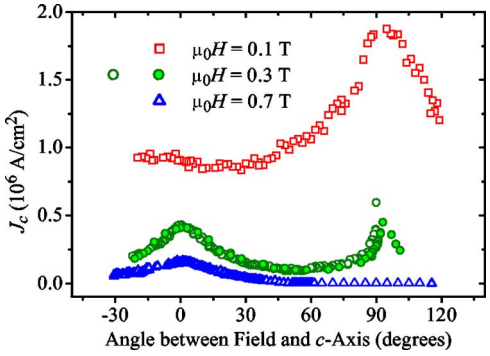

FIG. 9. (Color online) Angle dependences $J_c(H,\theta)$ for the K2 film at three different applied fields. Angular hysteresis at 0.3 T: solid and open symbols correspond to increasing and decreasing branches, respectively.

than the field of longitudinal vortex entry, $H_{c1}(\theta)$. (iv) For YBCO films with a degraded surface—i.e., without a peak effect—the $J_c(H\|ab)$ dependence may be scaled for an arbitrary angle in the field range $H_m^{\|}<H^{\|}<H_{cr}$ by the empirical relation

$$J_c(H,\theta)=\frac{J_c(H^{\perp},\theta=0)J_c(H^{\|},\theta=90^\circ)}{J_c(0)}, \qquad (22)$$

where $H^{\|}=H\sin\theta$.

Thus, the effects of transverse and longitudinal field components on the critical current seem to be independent and may be well described by the mechanism of prevailing pinning on out-of-plane ED's. Such a scaling is likely caused by a finite tilt stiffness of vortices. Indeed, above a certain threshold field $H_p(\theta)$, which depends on the field orientation, the vortex lines deflect from their initial positions parallel to dislocations. Vortex ends bend under the action of Lorentz force arising due to the Meissner current, which is induced by the longitudinal component of the magnetic field (Fig. 8).

The independent influence of transverse and longitudinal field components is well confirmed by comparing the measured field dependences $J_c(H,\theta\neq 0,90^\circ)$ without a peak effect with the recalculated ones from $J_c(H,\theta=0)$ and $J_c(H,\theta=90^\circ)$ by Eq. (22) (Fig. 7).

IV. ANGLE DEPENDENCE OF $J_c(H)$

The question to be answered is why the $J_c(\theta)$ behavior in YBCO films at a constant applied field appears to be very controversial and could not be consistently understood earlier. Indeed, it is known that different authors presented quite different results on the $J_c(\theta)$ behavior, showing either one maximum at $\theta=90^\circ$ and no maximum at $\theta=0$[6,32] or two maxima at $\theta=0$ and $\theta=90^\circ$.[4,25,33] The absence of a J_c maximum at $\theta=0$—i.e., at $H\|c$—in a number of experimental works was considered as unambiguous evidence against the ED pinning model. We are showing in this work that one or two maxima of $J_c(\theta)$ dependences can be easily observed experimentally under different experimental conditions for the same YBCO film. Furthermore, the different $J_c(\theta)$ behavior appears to be comprehensible only in our model of vortex pinning on normal cores of out-of-plane ED's, taking into account not only the magnetic field value, but also the thickness and surface roughness of YBCO films.

At sufficiently low field $H<H_m^{\perp}$ there should be no angle dependence of the critical current because of equal plateau levels $J_c(H,\theta)=J_c(0)$. In the field range $H_m^{\perp}<H<H_m^{\|}$ the angle dependence arises and it is governed solely by the field component perpendicular to the surface in accordance with Eq. (22), because the parallel field component is naturally less than $H_m^{\|}$ and $J_c(H^{\|},\theta=90^\circ)=J_c(0)$. $H^{\perp}$ is decreasing with θ rising and, therefore, $J_c(H=\text{const},\theta)$ is increasing according to Eq. (22) and the monotonic decreasing dependence of $J_c(H,\theta=0)$ (Fig. 6). Recalculation of $J_c(H^{\perp})$ to the dependence on θ results in a monotonic curve with a maximum at $H\|ab$ and a minimum at $H\|c$. So an increase of θ results in an effective decrease of magnetic field or, more exactly, magnetic induction (vortex density) in the film. The decrease leads to a shift of experimental curves toward higher fields and to a longer plateau at $\theta>0$.

At $H^{\|}>H_m^{\|}$ $J_c(H)$ according to Eq. (22) the steep decrease of $J_c(H,\theta=90^\circ)$ results in a second maximum of the angle dependence at $\theta=0$ observed for thicker films ($d\geqslant\lambda$) and a degraded surface (Fig. 9). The maximum becomes more pronounced at higher applied fields, while the maximum at $\theta=90^\circ$ becomes smaller but sharper. The heights of the two maxima equalize at the field at which $J_c(H\|c)$ and $J_c(H\|ab)$ plots are crossing over (Fig. 6) (0.3 T for the degraded K2 film). At $H=0.7$ T the peak at $H\|c$ is still observable, whereas in the vicinity of $\theta=90^\circ$ J_c appears to be less than 10 kA/cm^2 and cannot be measured by the ac magnetic susceptibility technique with sufficient accuracy.

In the intermediate-field range $J_c(\theta)$ exhibits a hysteretic behavior in the vicinity of $\theta=90^\circ$ (0.3 T, Fig. 10). After field cooling at $\theta=90^\circ$ and field rotation to $\theta=0^\circ$ and backwards the measured critical current at 90° reaches a lower value. Such a hysteresis is supposed to occur due to strong pinning on ED's.

V. DISCUSSION

As mentioned above, the model of vortex pinning in YBCO films proposed in Refs. 16–18 and developed in the

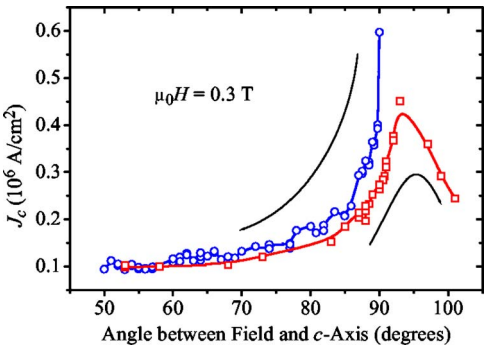

FIG. 10. (Color online) Angular hysteresis of the critical current at an intermediate parallel field for the K2 film.

present work is based on the dominant role of out-of-plane linear defects (e.g., edge dislocations). Rows of ED's form low-angle boundaries, which in turn form a nanostructure network in the films. However, the controversial absence of a $J_c(\theta)$ maximum at $H\|c$ in a certain field range in some experiments[6] led to ruling out this dislocation model. The main objective of this work is proving that the dislocations do play a major role in spite of a maximum absence at $\theta=0$. We have clearly shown that the J_c maximum at $H\|c$ does not appear only in the low field range (Fig. 9). This observation does not contradict our model, but complements the description of vortex pinning for any field direction and magnitude. It should be noted that the plateau value $J_c(H\to 0)$ is determined by pinning of a single vortex parallel to the c axis. Such vortices always exist in films due to a high demagnetization factor.[21]

The mechanisms of $J_c(H)$ decreasing above the plateau are essentially different for $\theta=0$ and $\theta=90°$. The $H_m^{\perp}$ value for $\theta=0$ is determined by the VLL accommodation function at the ED ensemble and can be rather low for perfect films with large single-crystal domains. For $\theta=90°$, $H_m^{\|}\approx H_p(0)$ is determined by surface Meissner currents induced by the parallel field, which deflect the ends of all vortices from dislocation cores and reduce the total pinning force. The field at which the Meissner current at the film surface is equal to the critical current in zero field (or at the plateau) is[33]

$$H_m^{\|}=\frac{4\pi\lambda}{c\tanh[d/(2\lambda)]}J_c(0)\approx\frac{8\pi\lambda^2}{cd}J_c(0). \tag{23}$$

The $J_c(H)$ dependence in an inclined field with parallel component $H^{\|}<H_m^{\|}$ is governed exceptionally by the component perpendicular to the film surface $H^{\perp}$ through the field dependence $J_c(H^{\perp},\theta=0)$. Thus, at low fields $H_m^{\perp}<H<H_m^{\|}$ pinning on ED's parallel to the c axis results in the single maximum of $J_c(\theta)$ at $H\|ab$ and a minimum at $H\|c$.

For very thin films ($d\ll\lambda$) there is a field range $H_m^{\|}<H<H_{c1}^{\|}$, in which both field components suppress the critical current independently [Eq. (22), Fig. 7], being conceived through the accommodation function for out-of-plane vortices and the decrease of pinned vortex lengths because of the Meissner current, respectively. Here, $H_{c1}^{\|}$ is the field of vortex entry into the film with account of anisotropy:

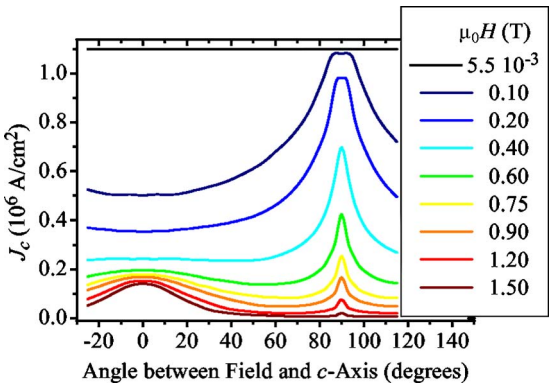

FIG. 11. (Color online) Evolution of the angle dependences with the applied field (from 0.0055 up to 1.5 T) calculated according to Eq. (22).

$$H_{c1}=\frac{2\phi_0}{\pi d^2\Gamma}\ln\left(\frac{d}{\xi_c}\right), \tag{24}$$

where $\Gamma=\lambda_c/\lambda_{ab}$ is the anisotropy parameter and $\xi_c(T)=\xi_0/(\Gamma\sqrt{\tau})$ is the c-axis coherence length. For YBCO, $\Gamma\approx 5-7$.[10]

In thicker films ($d\leqslant\lambda$) $H_m^{\perp}$, $H_m^{\|}$, and $H_{c1}^{\|}$ can be of the same order of magnitude. In this case a simplified approach of two independent depinning mechanisms by $H^{\perp}$ and $H^{\|}$ is not applicable.

For the as-grown films, the thickness of which reaches about λ, the observed J_c enhancement for $H\|ab$ (Fig. 6) can be explained by the interplay between electromagnetic pinning on the Bean-Livingston surface barrier and pinning on ED's. In the vicinity of $H_{c1}^{\|}$ the critical current density due to the electromagnetic mechanism only is[34]

$$J_c(H)=\frac{cdH}{4\pi^2\lambda^2}\left\{\arccos\left(\frac{H_m}{H}\right)^{1/2}-\left[\frac{H_m}{H}\left(1-\frac{H_m}{H}\right)\right]^{1/2}\right\}, \tag{25}$$

where $H_m=\pi\phi_0/(4d^2)$ is the field of metastable vortex appearance. The electromagnetic critical current increases with H until a second row of vortices is formed in the film. After the first row is completed, the critical current decreases abruptly as $H^{-1/2}$. The efficiency of the Bean-Livingston barrier is known to depend strongly on the surface quality. Since the surface of as-grown OMS films usually is rather smooth (in accordance with our atomic force microscopy data the peak-to-valley distance is as low as 2 nm in contrast to PLD films, where it is at least 20–30 nm), they exhibit the peak of J_c at $H\|ab$ (Fig. 6). The suppression of the peak effect after several thermal cycles (Fig. 6) may be explained by a surface degradation. $H_m^{\perp}$ and $H_m^{\|}$ get quite close after thermal cycling of the 300-nm-thick OMS film. $J_c(H)$ at $\theta=90°$ becomes steeper and the curves for $H\|c$ and $H\|ab$ orientations are crossing at $H_{cr}=0.34$ T for the K2 film. The crossing is not observed for the as-grown film.

The consistency of the dislocation pinning model is confirmed by Fig. 11, which presents the evolution of the angle dependences for the same film at different applied fields. The data for this figure are recalculated using all available $J_c(H)$

curves for the K2 film and interpolated. There is only the $J_c \| ab$ maximum at low fields $H < H_m^{\|}$. The field increase above $H_m^{\|}$ (0.3 T) leads to the emergence of another maximum at $J_c \| c$. At the further field increase the maximum at $J_c \| ab$ is sharpening and its height is reducing. The $J_c(H \| ab)$ shows hysteretic behavior. Therefore, the peak height and width change depend on the angle history. When the field rises well above H_{cr}, the maximum at $J_c(H \| ab)$ disappears. Thus, the field dependences crossing and disappearance of the peak effect are shown to have the same origin: the film surface roughness, which suppresses the surface barrier for entry and exit of longitudinal vortices and, as a matter of fact, facilitates the entry of transverse vortices.

The hysteretic behavior of $J_c(\theta = 90°)$ at $H \approx H_{cr}$ can be explained by a decrease of the number of parallel vortices after field rotation to the normal orientation and backwards. The surface barrier prevents entry of the longitudinal vortices, which are responsible for the electromagnetic pinning mechanism, but they have a chance to enter easily during the field rotation.

VI. CONCLUSIONS

Supercurrent transport phenomena are studied in epitaxial *c*-axis-oriented thin films of the HTS cuprate $YBa_2Cu_3O_{7-\delta}$ with high J_c (77 K) $\approx 10^6$ A/cm^2 by the four-probe transport technique, low-frequency ac magnetic susceptibility, and SQUID magnetometry. The complete self-consistent model of vortex pinning and supercurrent limitation is developed and discussed on the basis of transport current and magnetic measurement results. Rows of growth-induced out-of-plane edge dislocations forming low-angle boundaries are shown to play a key role in supercurrent transport phenomena. The evolution of angle dependences $J_c(\theta)$ with H is shown to be consistent with the model—i.e., with the dominant pinning on edge dislocations. New phenomena, the peak effect on $J_c(H \| ab)$ curves and the angular hysteresis of $J_c(\theta)$, are observed in the intermediate field range and discussed in terms of film thickness, surface quality, and orientation of the applied field. Thus, the following features are shown for the first time.

(i) The absence of a $J_c(H \| c)$ maximum of angle dependences does not contradict the dislocation pinning-transparency model. Moreover, the effect appears to be explained consistently by the model taking into account that only a perpendicular field component can enter the film at $H < H_p$.

(ii) There is a threshold field H_p, above which vortex ends are bending under the action of the Lorentz force due to the surface Meissner current and, hence, the longitudinal field component is emerging. The $J_c(H = \text{const}, \theta)$ dependence turns out to reveal the maximum at $H \| c$ only starting from the threshold field—i.e., at $H > H_p$.

(iii) The peak effect—i.e., $J_c(H \| ab)$ increase—is observed just above $H_m^{\|}$. The peak effect is assumed to be due to the surface barrier, which additionally pins parallel vortices, which try to escape from the film under the action of Lorentz force directed perpendicular to the film surface.

(iv) The entry and exit of parallel vortices in YBCO films with a rough surface—i.e., manufactured by the PLD technique or degraded after thermal cycling $300 \rightleftharpoons 77$ K—are essentially facilitated and the peak effect is gradually disappearing.

(v) The emergence of a single $J_c(\theta)$ peak, either at $H \| c$ or at $H \| ab$, or two peaks at both orientations of the applied field is determined not only by the film nanostructure, but also by the value of the applied magnetic field, the film thickness, and the film surface state.

(vi) The angle dependence of the critical current exhibits a hysteretic behavior in the vicinity of $H \| ab$, that is, $J_c(H, \theta)$ depends on the way the particular state is achieved. The hysteresis arises due to the surface barrier for entry and exit of parallel vortices.

ACKNOWLEDGMENTS

The authors would like to express their deep gratitude to Dr. A. L. Kasatkin for many fruitful discussions and to Dr. V. L. Svetchnikov and Professor H. W. Zandbergen for their contribution to electron microscopic film characterization, and to G. S. Mogil'nyi for help with the x-ray diffractometry. This work is supported through Project No. 036-2003 IMP/NASU and the Australian Research Council.

*Electronic address: pan@imp.kiev.ua

[1] P. Chaudhari, R. H. Koch, R. B. Laibowitz, T. R. McGuire, and R. J. Gambino, Phys. Rev. Lett. **58**, 2684 (1987).

[2] G. W. Crabtree, J. Z. Liu, A. Umezawa, W. K. Kwok, C. H. Sowers, S. K. Malik, B. W. Veal, D. J. Lam, M. B. Brodsky, and J. W. Downey, Phys. Rev. B **36**, R4021 (1987).

[3] V. M. Pan, A. L. Kasatkin, V. L. Svetchnikov, and H. W. Zandbergen, Cryogenics **33**, 21 (1993).

[4] B. Roas, L. Schultz, and G. Saemann-Ischenko, Phys. Rev. Lett. **64**, 479 (1990).

[5] Ch. Jooss, R. Warthmann, and H. Kronmüller, Phys. Rev. B **61**, 12433 (2000).

[6] C. J. van der Beek, M. Konczykowski, A. Abal'osheva, I. Abal'osheva, P. Gierlowski, S. J. Lewandowski, M. V. Indenbom, and S. Barbanera, Phys. Rev. B **66**, 024523 (2002).

[7] J. L. MacManus-Driscoll, S. R. Foltyn, Q. X. Jia, H. Wang, A. Serquis, L. Civale, B. Maiorov, M. T. Hawley, V. P. Maley, and D. E. Peterson, Nat. Mater. **3**, 439 (2004).

[8] A. I. Kosse, Yu. E. Kuzovlev, G. C. Levchenko, Yu. V. Medvedev, A. Yu. Prokhorov, V. A. Khokhlov, and P. N. Mikheenko, JETP Lett. **78**, 379 (2003).

[9] L. Civale, A. D. Marwick, T. K. Worthington, M. A. Kirk, J. R. Thompson, L. Krusin-Elbaum, Y. Sun, J. R. Clem, and F. Holtzberg, Phys. Rev. Lett. **67**, 648 (1991).

[10] J. Z. Liu, Y. X. Jia, R. N. Shelton, and M. J. Fluss, Phys. Rev. Lett. **66**, 1354 (1991).

[11] L. Civale, B. Maiorov, A. Serquis, J. O. Willis, J. Y. Coulter, H. Wang, Q. X. Jia, P. N. Arendt, J. L. MacManus-Driscoll, M. P. Maley, and S. R. Foltyn, Appl. Phys. Lett. **84**, 2121 (2004).
[12] G. Blatter, M. V. Feigel'man, V. B. Geshkenbein, A. I. Larkin, and V. M. Vinokur, Rev. Mod. Phys. **66**, 1125 (1994).
[13] V. F. Solovjov, V. M. Pan, and H. C. Freyhardt, Phys. Rev. B **50**, 13724 (1994).
[14] B. Maiorov, B. J. Gibbons, S. Kreiskott, V. Matias, Q. X. Jia, T. G. Holesinger, and L. Civale, IEEE Trans. Appl. Supercond. **15**, 2582 (2005).
[15] A. V. Silhanek, L. Civale, and M. A. Avila, Phys. Rev. B **65**, 174525 (2002).
[16] Yu. V. Fedotov, S. M. Ryabchenko, E. A. Pashitskii, A. V. Semenov, V. I. Vakaryuk, V. S. Flis, and V. M. Pan, Physica C **372-376**, 1091 (2002).
[17] Yu. V. Fedotov, S. M. Ryabchenko, E. A. Pashitskii, A. V. Semenov, V. I. Vakaryuk, V. M. Pan, and V. S. Flis, Low Temp. Phys. **28**, 172 (2002).
[18] V. M. Pan, E. A. Pashitskii, S. M. Ryabchenko, V. A. Komashko, A. V. Pan, S. X. Dou, A. L. Kasatkin, A. V. Semenov, C. G. Tretiatchenko, and Yu. V. Fedotov, IEEE Trans. Appl. Supercond. **13**, 3714 (2003).
[19] J. R. Clem and A. Sanchez, Phys. Rev. B **50**, 9355 (1994).
[20] M. Wurlitzer, M. Lorenz, K. Zimmer, and P. Esquinazi, Phys. Rev. B **55**, 11816 (1995).
[21] A. V. Pan, Y. Zhao, M. Ionescu, S. X. Dou, V. A. Komashko, V. S. Flis, and V. M. Pan, Physica C **407**, 10 (2004).
[22] B. Dam, J. M. Huijbregtse, F. C. Klaassen, R. C. F. van der Geest, G. Doornbos, J. H. Rector, A. M. Testa, S. Freisem, J. C. Martinez, B. Stäuble-Pümpin, and R. Griessen, Nature (London) **399**, 439 (1999).
[23] E. Zeldov, A. I. Larkin, V. B. Geshkenbein, M. Konczykowski, D. Majer, B. Khaykovich, V. M. Vinokur, and H. Shtrikman, Phys. Rev. Lett. **73**, 1428 (1994).
[24] S. K. Streiffer, B. M. Lairson, C. B. Eom, B. M. Clemens, J. C. Bravman, and T. H. Geballe, Phys. Rev. B **43**, 13007 (1991).
[25] V. M. Pan, A. L. Kasatkin, V. S. Flis, V. A. Komashko, V. L. Svetchnikov, A. V. Pronin, C. L. Snead, M. Suenaga, and H. W. Zandbergen, J. Low Temp. Phys. **117**, 1537 (1999).
[26] E. A. Pashitskii and V. I. Vakaryuk, Low Temp. Phys. **28**, 11 (2002).
[27] K. Merkle, Interface Sci. **2**, 311 (1995).
[28] V. Svetchnikov, V. Pan, Ch. Traeholt, and H. Zandbergen, IEEE Trans. Appl. Supercond. **7**, 1396 (1997).
[29] G. Ghigo, D. Botta, A. Chiodoni, R. Gerbaldo, L. Gozzelino, B. Minetti, C. Camerlingo, and C. Giannini, in *Proceedings of the 10th International Workshop on Critical Currents, Göttingen, Germany, 2001*, edited by C. Jooss, (Universität Göttingen, Göttingen, 2001), p. 100.
[30] E. Mezzetti, R. Gerbaldo, G. Ghigo, L. Gozzelino, B. Minetti, C. Camerlingo, A. Monaco, G. Cuttone, and A. Rovelli, Phys. Rev. B **60**, 7623 (1999).
[31] B. E. Warren and B. L. Averbach, J. Appl. Phys. **21**, 595 (1950).
[32] Yu. V. Fedotov, E. A. Pashitskii, S. M. Ryabchenko, V. A. Komashko, V. M. Pan, V. S. Flis, and Yu. V. Cherpak, Low Temp. Phys. **29**, 630 (2003).
[33] Yu. V. Cherpak, V. A. Komashko, S. A. Pozigun, A. V. Semenov, E. A. Pashitskii, and V. M. Pan, IEEE Trans. Appl. Supercond. **17**, 2783 (2005).
[34] G. Stejic, A. Gurevich, E. Kadyrov, D. Christen, R. Joynt, and D. C. Larbalestier, Phys. Rev. B **49**, 1274 (1994).